AD-A143 967 A STUDY OF LONG AEROSOL INITIATED LASER INDUCED AIR BREAKDOWN PLASMAS(U) NAVAL RESEARCH LAB WASHINGTON DC R E PECHACEK ET AL. 29 JUN 84 NRL-MR-5362 1/1

UNCLASSIFIED F/G 20/9 NL

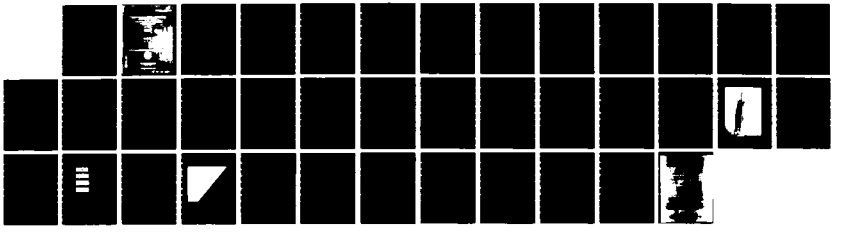

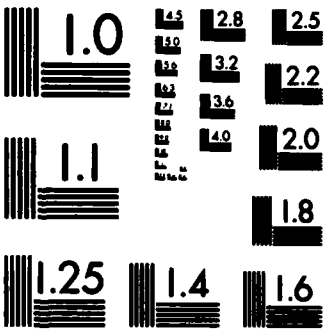

MICROCOPY RESOLUTION TEST CHART
NATIONAL BUREAU OF STANDARDS-1963-A

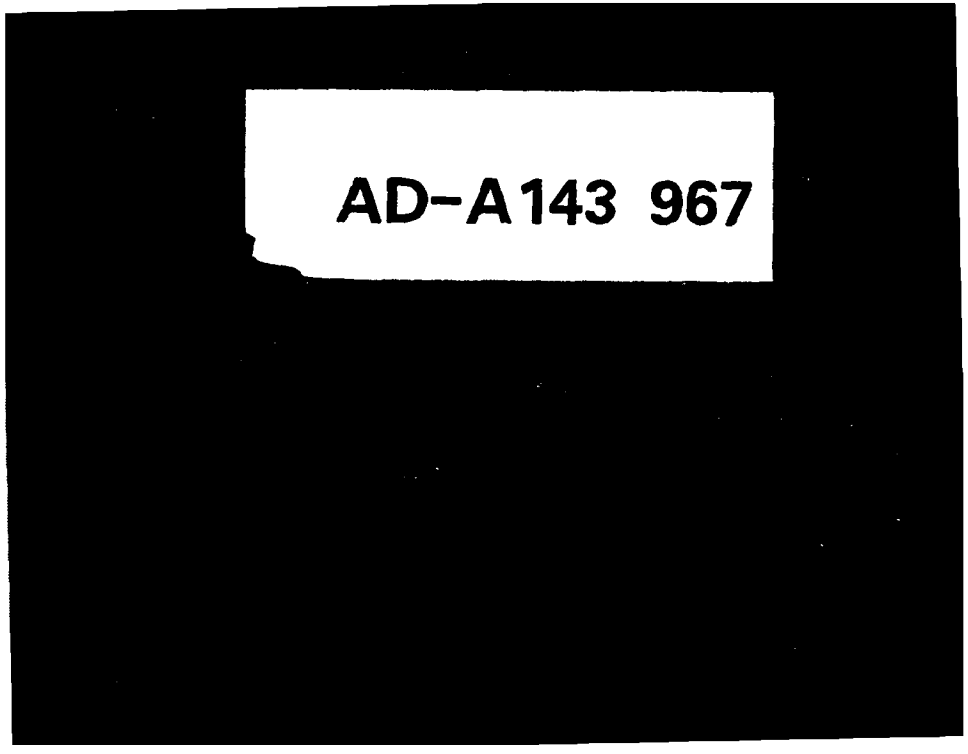
AD-A143 967

SECURITY CLASSIFICATION OF THIS PAGE

REPORT DOCUMENTATION PAGE

1a REPORT SECURITY CLASSIFICATION UNCLASSIFIED	1b RESTRICTIVE MARKINGS
2a SECURITY CLASSIFICATION AUTHORITY	3 DISTRIBUTION/AVAILABILITY OF REPORT Approved for public release; distribution unlimited.
2b DECLASSIFICATION/DOWNGRADING SCHEDULE	
4 PERFORMING ORGANIZATION REPORT NUMBER(S) NRL Memorandum Report 5362	5. MONITORING ORGANIZATION REPORT NUMBER(S)
6a NAME OF PERFORMING ORGANIZATION Naval Research Laboratory 6b. OFFICE SYMBOL (If applicable) Code 4763	7a. NAME OF MONITORING ORGANIZATION
6c ADDRESS (City, State and ZIP Code) Washington, DC 20375	7b. ADDRESS (City, State and ZIP Code) AUG 3 1984
8a NAME OF FUNDING/SPONSORING ORGANIZATION ONR and NAVSEA 8b OFFICE SYMBOL (If applicable)	9. PROCUREMENT INSTRUMENT IDENTIFICATION NUMBER
8c ADDRESS (City, State and ZIP Code) Arlington, VA 22217 Washington, DC 20362	10. SOURCE OF FUNDING NOS. PROGRAM ELEMENT NO.: 61153N, 63514N PROJECT NO.: S-0384-SL TASK NO: RR011-09-41, 24769 WORK UNIT NO: DN380-235
11 TITLE (Include Security Classification) (See page ii)	
12 PERSONAL AUTHOR(S) Pechacek, R.E., Raleigh, M., Greig, J.R., Murphy, D.P., and Camelio, F.*	
13a TYPE OF REPORT Interim 13b. TIME COVERED FROM 10/82 TO 9/83	14 DATE OF REPORT (Yr., Mo., Day) June 29, 1984 15 PAGE COUNT 38
16. SUPPLEMENTARY NOTATION *US Naval Academy, Annapolis, MD This work was supported by the Office of Naval Research and the Naval Sea Systems Command.	
17 COSATI CODES FIELD / GROUP / SUB. GR.	18 SUBJECT TERMS (Continue on reverse if necessary and identify by block number) Laser induced Air breakdown neodymium

19 ABSTRACT (Continue on reverse if necessary and identify by block number)

Results from three separate experiments on aerosol initiated, laser induced, air breakdown are described. The purpose of these experiments was to determine the maximum length of air breakdown plasma that can be created with a given laser pulse. Two separate Nd:glass lasers were used; the first produced an output pulse of 30 J in 60 ns and the second produced 200 J in 4 ns. Both pulses were at the wavelength of 1.06 μm. Two of the experiments used the aerosol produced by burning black gunpowder in the atmosphere which gave a mean particle size of ~ 0.5 μm. The third experiment attempted to use ragweed pollen with a mean particle size of ~ 10 μm, but these particles could not be adequately dispersed and no useful results were obtained. Using the black powder, aerosol densities from that naturally present in the laboratory (a scattering length of ~ 64 m) to that necessary to give a scattering length at 1.06 μm of ~ 2 m, were achieved in a controlled, reproducible manner. The maximum length of breakdown plasma actually observed was ~ 10 m, and this was achieved using the 50 GW laser pulse. The intensity threshold for causing aerosol

(Continues)

20 DISTRIBUTION/AVAILABILITY OF ABSTRACT UNCLASSIFIED/UNLIMITED ☒ SAME AS RPT ☐ DTIC USERS ☐	21 ABSTRACT SECURITY CLASSIFICATION UNCLASSIFIED
22a NAME OF RESPONSIBLE INDIVIDUAL R. E. Pechacek	22b TELEPHONE NUMBER (Include Area Code) (202) 767-2077 22c OFFICE SYMBOL Code 4763

DD FORM 1473, 83 APR EDITION OF 1 JAN 73 IS OBSOLETE

SECURITY CLASSIFICATION OF THIS PAGE

11. TITLE (Include Security Classification)

A Study of Long Aerosol Initiated Laser Induced Air Breakdown Plasmas

19. ABSTRACT

induced air breakdown was the same for both laser pulses, ~ 4×10^9 watts/cm^2, but the 50 GW pulse produced smaller, more numerous breakdown plasmas than the 0.5 GW laser pulse. The data obtained fit easily to a simple theory assuming Gaussian laser beams and diffraction limited optics (a good approximation for these experiments), and this theory predicts that laser induced, aerosol initiated, air breakdown can readily be achieved over lengths in excess of 100 m in an aerosol contaminated atmosphere using the 50 GW laser pulse.

CONTENTS

INTRODUCTION 1

DESCRIPTION OF THE EXPERIMENT 2

PROPERTIES OF THE BLACK POWDER SMOKE AEROSOL 4

DETERMINATION OF AEROSOL DENSITY BY LIGHT SCATTERING 5

RESULTS OF THE EXPERIMENT 7

RESULTS OF A VERY HIGH INTENSITY LASER EXPERIMENT 10

DISCUSSION AND CALCULATION OF MAXIMUM BREAKDOWN LENGTHS.. 11

CONCLUSIONS 15

ACKNOWLEDGMENTS 16

APPENDIX I 18

REFERENCES 30

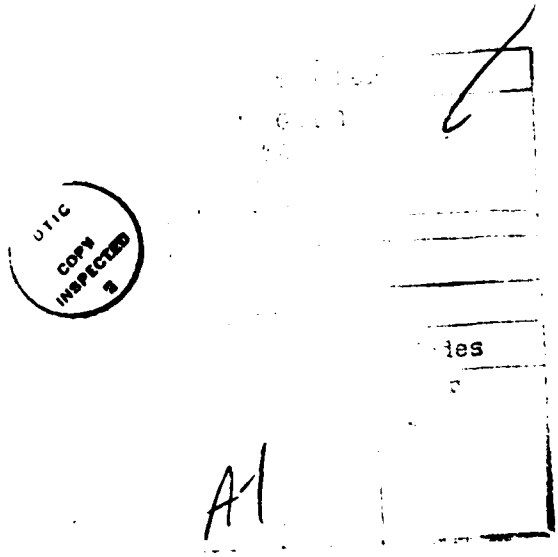

A STUDY OF LONG AEROSOL INITIATED LASER INDUCED AIR BREAKDOWN PLASMAS

INTRODUCTION

Partially conducting, reduced density channels in the atmosphere can be produced along predictable paths by high energy focussed laser beams. These channels are interesting for at least two reasons: (i) If high energy particle beams are to propagate at atmospheric pressure, they will have to propagate in, and they will produce, reduced density channels. (ii) A high voltage electric discharge will follow the path of a reduced density channel. Long, predictably located, electric discharges, guided along a laser produced channel, provide a systematic means of studying lightning phenomena. The highly conductive afterglow plasmas of these precisely located electric discharges have been used as radio frequency antennas to transmit and receive information.[1]

For several years, partially conducting, reduced density channels in the atmosphere have been produced at NRL using both Nd/glass and CO_2 lasers. These lasers produce channels that are reduced in density to about 40% of ambient density and have conductivities in the range of 1×10^6 Hz. An electric discharge guided along the laser produced channel further reduces its density to about 10% of ambient. Longer laser produced channels are possible in aerosol seeded air than are possible in clean air. Laser produced plasma channels as long as 10 meters have been created in air seeded with aerosols produced by burning black powder.

The purpose of this present work is to investigate the dependence of the length of the laser produced plasma channel on aerosol density, system focal length, and laser energy, in order to design future experiments with even longer channels. The experimental method in this work is to correlate the photographically recorded plasma channel lengths with the above mentioned parameters. The result of this correlation is a determination of the aerosol density range that is useful in increasing the plasma channel length and a determination of the threshold of laser intensity on the aerosol particles that produces sufficient ionization to cause breakdown.

Manuscript approved April 4, 1984.

DESCRIPTION OF THE EXPERIMENT

The apparatus for the experiment is shown schematically in Fig. 1. An approximately 30 Joule, 60 nsec FWHM, 1.06 micron, laser pulse, after passing through power and energy monitors, is turned by a prism, focussed by a 5 to 10 meter focal length lens, and finally turned again by a prism into a 10 meter long aerosol chamber. The focus of the optical system is placed at the midpoint of the chamber. Open shutter cameras photograph the laser produced plasma-channel to record its length. The aerosol density is known as a function of time from previous measurements which used an optical multichannel analyzer to measure light scattered by the aerosols from an argon ion laser beam.

Following in this section is a description of the experiment chamber and the aerosol generating system, a description of the measurement of the plasma channel length, and a description of the aerosol density measuring system. Finally, a brief description is given of experiments using 10 micron diameter pollen particles instead of black powder smoke as the breakdown enhancing aerosol.

A schematic diagram of the experiment chamber is shown in the upper part of Fig. 1. The chamber consists of six, 50 cm diameter by 3.05 meter long sections of a hard paper tube used in the building industry for casting concrete columns. The tubes are joined into two approximately 10 meter long sections located side by side, near the ceiling of a large room, as shown in the photograph of Fig. 2. The 10 meter sections are joined together at each end so that air can circulate continuously through the system. The upper tube is the laser-aerosol interaction region. The ends of this tube are closed by a combination turning prism-window on one end and a Brewster angle blue glass beam dump on the other. A ten centimeter high acrylic window provides visual access along almost the entire length of the upper tube for photographing the laser produced plasma channel. The lower tube contains a fan to continuously circulate the aerosol-air mixture, and a port connected to a pump that maintains the chamber at a pressure of about one Torr below ambient pressure. The flow rate is 1.6 meters/second or one revolution per 12.4 seconds. One end of the lower tube is sealed. The other end has a door for

introducing the black powder and, just inside the door, an asbestos plate on which the powder is burned. To fill the system, 1.5 grams of blackpowder is ignited with a hot nichrome wire.

The laser induced breakdown experiments are undertaken by focussing the pulsed Nd/glass laser beam into the center of the aerosol chamber. Three parameters are varied: laser energy, lens f-number, and aerosol density. Three focussing lenses are used, 5, 7.5, and 10 meter focal lengths, corresponding to f-numbers of 138, 235, and 360. The energy of the laser pulses is varied from 10 to 30 Joules. The energy of each pulse was inferred from its peak intensity, as measured on a fast, high current, ITT F100 photodiode. Calorimeter readings and laser power supply settings are not a good indication of the energy in the laser pulse because of target interactions with the laser. Pre-lasing due to target interaction, in this case the aerosols, is an effect that causes difficulty only with the short focal length experiments.

The raw data in this experiment are open shutter photographs of the laser produced plasma channels that can be accurately scaled to determine their length. The cameras are located 7.65 meters from the centerline of the experiment chamber, view the chamber at a right angle to its centerline, and have focal lengths of 50 and 162 mm. To calibrate the photographs, a scale with 10 cm increments is marked on the chamber, just above the viewing window. These 10 cm marks are evident in Fig. 2. The plasma channel lengths can easily be determined within 2 cm for plasmas produced through the 7.5 and 10 meter focal length lenses. With the 5 meter focal length lens, the plasmas are so intense that light scattered from the windows saturates the film, hiding the detail of the spark. Since the 5 meter focal length lens produces only relatively short plasmas, there is a loss of accuracy only for the less interesting data.

The aerosol density in the chamber decreases exponentially from the time that the black powder is ignited until it reaches the density of aerosols in laboratory air. From experiment to experiment, the aerosol density is varied by simply waiting until the desired level is reached. The initial aerosol density is determined from argon ion laser scattering measurements that are described in the next section. The laser attenuation length corresponding to the initial density is 2.5 meters. The aerosol density decay time is measured

to be about 8 minutes, and data is taken from 10 seconds after black powder ignition to 10,000 seconds after ignition. At this later time, the aerosol density in the chamber is the same as that of laboratory air.

Besi black powder smoke aerosols, attempts were made to study laser discharges in air laden with ragweed pollen. Ragweed pollen grains are approximately spherical and about 10 microns in diameter: over ten times the diameter of black powder smoke particles. It was thought that the larger particles might have a considerably lower threshold of laser intensity for producing breakdown. Unfortunately, it was not possible to properly disperse the pollen and the agglomerates settled out and stuck to the chamber walls too fast to make a density determination. The few discharges that were made with the pollen aerosol were not as long as corresponding discharges with black powder smoke.

PROPERTIES OF THE BLACK POWDER SMOKE AEROSOL

When black powder (75% KNO_3, 15% charcoal, and 10% sulphur) is burned, a dense white smoke is evolved that consists chiefly of potassium sulphate, potassium thiosulphate, and potassium carbonate. An idea of the complexity of the black powder reaction is given by its chemical equation:

$$74KNO_3 + 30S + 16C_6H_2O(\text{charcoal}) \rightarrow 56CO_2 + 14CO$$
$$+ 3CH_4 + 2H_2S + 4H_2 + 35N_2 + 19K_2CO_3 + 7K_2SO_4$$
$$+ 2K_2S + 8K_2S_2O_3 + 2KCNS + (NH_4)_2CO_3$$
$$+ C + S + 665 \text{ kcal/kg} \quad . \qquad (1)$$

This equation is based on the analysis of reaction products and may vary under different burning conditions and compositions. (See Reference 2.) Analysis of this reaction shows that 62% of the initial weight of the black powder becomes particulate material after burning.

Microscopic examination of smoke particles that had settled on a glass surface indicates a particle size distribution that is sharply peaked about one micron in diameter. However, this value leads to conclusions that are either unphysical or in conflict with other observations: viz, it implies that

the scattering crossection for argon ion laser light is ten times the particle silhouette, and that the particles should have about equal cross sections for scattering both .5145 micron argon ion laser light and 1.06 micron Nd/glass laser light. The visual measurement of the particles, therefore, is disregarded on the grounds that diffraction effects caused errors in the measurements or that the particles that settle out are not representative of the total aerosol population. Based on preliminary electron microscope measurements and on the observed relative magnitude of the scattering cross section for .5143 micron and 1.06 micron light a more reasonable value for the average particle diameter is 0.5 micron, and this is the assumed value for the diameter of the average blackpowder aerosol particle.

An upper limit on the initial aerosol number density can be determined from the chamber volume, average particle diameter, and amount of powder burned. For a chamber volume of 3.7 cubic meters, 1.5 grams of powder, and an assumed particle diameter of 0.5 microns the maximum possible initial density is 1.5×10^6 cm^{-3}. The index of refraction of the aerosol particles is that of the constituent potassium salts, about 1.5, and the specific gravity of the particles is about 2.5.

DETERMINATION OF AEROSOL DENSITY BY LIGHT SCATTERING

The experiment chamber is not air tight and is maintained slightly below ambient pressure. A result of this constant replacement of the air in the chamber is that its aerosol density decreases exponentially from its initial value to that of the laboratory air, and this change in the aerosol content is faster than any changes in the aerosol size distribution caused by settling of the larger particles. To determine the aerosol density in the chamber as a function of time, light scattered out of the beam from a cw argon ion laser is recorded, as a function of time, from the time of ignition of the black powder to the time that the aerosol density in the chamber approaches that of the ambient air. Figure 3 is a schematic diagram of this experimental arrangement.

There are three parameters to be determined: the initial aerosol density, the decay rate of the density, and the total scattering cross section of the aerosol particles. The density decay rate is straight forwardly determined,

as it is the decay rate for the scattered light. The product of the density and the total cross section is determined at a single instant of time when a maximum occurs in the scattered light signal. Since the cross section is assumed to be a constant and the density to decrease exponentially, the density-cross section product is determined for all time. If other measurements can determine the cross section or the initial density, the density as a function of time is determined.

Equation (2) is the expression that governs the size of the light signal detected at time, t, due to light scattered from a region located at a position, z, in a volume that is being irradiated by a beam whose intensity at z=0 is I_0.

$$I(z,t) = I_0 n(t)(d\sigma/d\Omega)\Delta\Omega e^{-n(t)\sigma z} \qquad (2a)$$

$$n(t) = n_0 e^{-\gamma t} \qquad (2b)$$

In Equation (2), n(t) is the exponentially decaying density function, γ is its decay rate, and $(d\sigma/d\Omega)\Delta\Omega$ is the scattering cross section for scattering the laser light into the detector optics. The exponential in Eq. (2a) accounts for the attenuation of the laser beam by the aerosols. Equation (2a) has a maximum at the value of t given by

$$n(t)\ \sigma\ z = 1 \qquad (3)$$

Since the values of γ and t, at the maximum of I(z,t), are found from the scattered light record, and since z is determined by the experimental set-up, $n_0\sigma$ is determined absolutely; even though only relative intensity measurements are made.

Figure 4 is a graph of the scattering signal measurements made at the three axial positions along the aerosol chamber shown in Figure 3. The measurements are made at three minute intervals and recorded on an optical multichannel analyzer. The data points are compared to graphs of Eq. (2a) with γ equal to 0.12 $minute^{-1}$, $n_0\sigma$ equal to 0.4m^{-1}, and z equal to 4.1, 5.25, and 6.3 meters. The value of $n_0\sigma$ is determined from the maxima of the curves

through the data points and γ is determined from the slope of the curves at late time.

If the initial aerosol density from the previous section is used with the measured value of $n_0\sigma$ to calculate σ, the result is a cross section of 2.6×10^{-9} cm^2. This value is 1.3 times the silhouette of a 0.5 micron diameter particle, a rather low value according to Mie theory.[3] The separate evaluation of n_0 and σ is interesting because it is a check on the efficiency of the aerosol production. On the other hand, it is only academic, since the important quantity is the attenuation of the laser beam by the aerosol, and this depends on the product of n_0 and σ.

RESULTS OF THE EXPERIMENT

The organization of this section is as follows: (i) The experimental data is presented. (ii) The more meaningful data is selected for further discussion. (iii) The useful aerosol density range is determined. (iv) Attenuation of the laser beam by the aerosols is determined to be negligible. (v) From the known intensity distribution of a focussed Gaussian beam, the threshold breakdown intensity I_{bd}, is determined.

Appendix I is a table of the 48 laser shots fired into the aerosol chamber for this experiment. For each shot the following are given: shot number, optical system focal length and f-number, time interval between firing the laser and black powder ignition, laser energy, plasma channel length, and the channel length per unit laser energy. The same data are condensed in Table I. This table is a matrix indexed by the three values of f-number and four time intervals. In the squares are the minimum, the maximum, and the average values of the breakdown channel length per unit energy that correspond to laser pulses fired with the specified aperture and during the specified time interval.

There is a correlation in the data of Appendix I between aperture and laser energy: lower energy for lower f-number. The reason for this correlation is the interaction between the laser and the target aerosols that degrades the energy in the Q-switched pulse and is more severe at lower f-numbers.

It is apparent from the table that L' (the plasma length per unit laser energy) is greatest for the aerosol densities that occur for T (the time after black powder ignition) between 100 and 1400 seconds. It is also apparent that the values of L' for T equal to 10 seconds are inconsistent, or at least not simply related to the other values on the table. The reason for this inconsistency is that the aerosol is created at one end of the chamber and requires many seconds to evenly distribute itself. The values for T equal to 10 seconds are not representative of a uniform aerosol density, as are the other values. The values of L' for T greater than 1400 seconds are representative of a laser induced breakdown in laboratory air, rather than an aerosol enhanced breakdown. In the range of T between 10 and 100 seconds, the aerosol density is high enough to seriously attenuate the laser beam before the beam reaches focus. It is the region of T that is between 100 and 1400 seconds and its corresponding aerosol density range that produces the longest discharges. This is the range that is interesting and it is the data in this range that is analyzed further.

The first thing to notice about the discharge lengths in this 100 to 1400 second region is that, as scattered as the data seems to be, there is no correlation between the time of the discharge and its length. (See Appendix I.) Between 100 and 1400 seconds after the black powder ignition there is a factor of five reduction in the aerosol density: from 1.2×10^{6} to 2.4×10^{5} cm^{-3} for the assumed 0.5 micron particle size. If the Nd/glass laser beam were attenuated by the aerosol as the argon ion laser is, the longer discharges would occur at later times, when the attenuation is less, and the values of I_{bd} recorded at later times would be higher. That the Nd/glass laser beam is not attenuated is consistent with the assumed 0.5 micron particle size that puts the scattering process in the regime where the scattering cross section varies inversely with a power of the wavelength that is between two and four. The attenuation length for 1.06 micron radiation in this density range varies, at worst, from 13 to 64 meters, much longer than the five meter half length of the experiment chamber, and the corresponding variation in intensity is, at most, ± 15%.

Figure 5 affirms that the Nd/glass laser beam is not strongly attenuated by the aerosol. The figure shows four photographs of laser induced breakdown plasmas with the 10 meter focal length lens system: The first is without the

aerosol and is therefore very short. It does, however, locate the focal point of the optical system. The remaining three photographs are shots with the aerosol present. These three show that the laser induced plasma is located symmetrically about the focal region. If the laser beam were attenuated, the discharge would extend further toward the laser from focus than away from it.

To determine the threshold intensity for laser breakdown, the intensity distribution of the focussed Nd/glass laser beam must be used. The TEM_{oo} mode of the laser produces a very nearly Gaussian beam. (Such a beam has an intensity that varies radially as $I\exp(-r^2/r_o^2)$, where r_o is the nominal radius of the beam and I is the on-axis intensity. A property of the Gaussian function is that $I\pi r_o^2$ is the total power of the beam.) In the region beyond a focussing lens, the on-axis intensity as a function of axial position is given by the following function:

$$I(z) = I_o \frac{N^2(1+N^2)^{-1}}{(z/R_o - N^2(1+N^2)^{-1})^2 + N^2(1+N^2)^{-2}} \qquad (4a)$$

$$N = \pi a^2/\lambda R_o \qquad (4b)$$

where I_o is the intensity at the lens, R_o is the radius of curvature of the beam phase front immediately after the lens, N is proportional to the optical system Fresnel number, λ is the laser wavelength, and a is the beam radius at the lens.[4] Table II contains the values of these parameters for the three optical systems that were used. If Equation (4a) is evaluated at the values of z and I_o that correspond to the extremities of the laser induced plasma and the energy of the laser pulse, the resulting value of I(z) is the threshold intensity for breakdown. In all cases, N is very large and is neglected. With I_o expressed in terms of the laser pulse energy, the pulse duration (60×10^{-9} seconds), and the entrance area, and with $R_o/2a$ expressed as the f-number, Eq. (4a) is rearranged as

$$1 = 0.29\, f\sqrt{E}\, [I_{bd}]^{-1/2}, \qquad (5)$$

where l is the total length (i.e., 2z), in meters, of the laser induced plasma, E is the laser pulse energy in Joules, and I_{bd} is the breakdown intensity threshold in GW/cm^2. The breakdown intensity threshold is found from the data by (i) plotting the observed laser induced plasma lengths against their corresponding products of f-number and square root of pulse energy, (ii) finding the straight line through the origin that best fits these points, and (iii) evaluating Eq. (5) along this line and solving for I_{bd}. Figure (6) shows this plot and the "best fit" straight line to the f=235 and the f=360 data. The slope of this line corresponds to a laser breakdown intensity of 4.0×10^9 W/cm^2.

In summary, the density of black powder aerosols that extends the laser induced plasma lengths is between $.2 \times 10^5$ and 2.4×10^5 cm^{-3} (for an assumed particle diameter of 0.5 microns) and the threshold intensity for air breakdown in the aerosol atmosphere is 4×10^9 W/cm^2.

RESULTS OF A VERY HIGH INTENSITY LASER EXPERIMENT

Figure (7) is a photograph of a 10 meter long laser induced plasma that was made with a 200 Joule, 4 nanosecond pulse from a Nd/glass laser. The beam is focussed with a pair of lenses that produce a 17 meter focal length and an f-number of 213. The breakdown intensity threshold is estimated to be 4.5×10^9 W/cm^2. The aerosol is produced by burning 9.4 grams of black powder in a long corridor. The resulting maximum aerosol density is 1.1×10^{-7} $gram/cm^3$, and it produces an attenuation length of 11 meters for .6328 micron He-Ne laser radiation.

Figure (8) is a schematic diagram of the experimental layout. Because the experiment is conducted in a long corridor, it is impossible to view the entire interaction length from a 90 degree position. In order to accurately measure the plasma length, lights, at one meter intervals as shown in Figures (7) and (8), are strung along the left wall of the corridor. The position of the lights relative to distance along the optical axis is calibrated by a photograph showing both the lights and a string with one meter markers stretched along the optical axis. In Figure (7), the intersection between the optical axis and the line between the first scale mark and the first light is nine meters from the last focussing lens. Correspondingly, the intersection

of optical axis and the line joining the thirteenth light and scale mark is 21 meters from the lens.

Two things, besides its remarkable length, differentiate the plasma made by the 200 Joule, 4 nanosecond laser pulse from the plasma made by the 30 Joule, 60 nanosecond laser pulse: (i) The former is almost entirely upstream from the laser beam focal position, while the latter is centered about the focal position. The laser induced plasma of Figure (7) lies eight meters upstream of focus and two meters downstream. (ii) The plasma induced by the 200 Joule, 4 nanosecond laser pulse is extremely uniform compared to the lower power laser induced plasma, which has many isolated plasma regions along its length. The reason for the first difference is probably that the higher power laser ionizes the air in the focal region to such a high conductivity that the beam is almost entirely attenuated. The reason for the second difference may be as follows: the energy absorbed in the ionized gas around a single aerosol particle increases with the third or fourth power of time.[5] In the long, low power laser pulses, each individual plasma has time to grow and to absorb a much higher energy than in the high power case. These large plasma volumes may shadow downstream regions of the beam, causing gaps in the plasma brightness.

DISCUSSION AND CALCULATION OF MAXIMUM BREAKDOWN LENGTHS

A short focal length lens converges a laser beam so rapidly that the length of the biconical focal region that has an intensity above the threshold for producing optical breakdown is very short. As the focal length is increased, the breakdown region increases in length until a point is reached where diffraction begins to reduce beam convergence. Increasing the focal length beyond this point decreases the breakdown region, and, if the focal length is increased enough, the breakdown region will vanish. Somewhere between these extremes is an optimal optical system, which is the subject of this section.

The breakdown length is a function of several parameters: (i) The laser power, P_o, measured in watts. (ii) The threshold for optical breakdown, I_{bd}, which was determined for a black powder aerosol atmosphere in an earlier section to be 4×10^9 watts/cm^2. (iii) The radius of curvature of the laser

beam phase surface as the beam leaves the last optical interface. This length, R_o, is the same as the lens focal length for the case of a parallel beam incident on a simple lens. (iv) The wavelength of the incident radiation, λ. The longer the wavelength, the more important are the diffraction effects. (v) The Fresnel number, N, defined in Equation (4b), which gives a measure of the importance of diffraction. The smaller the Fresnel number, the more important are diffraction effects. (vi) The attenuation constant for the least amount of aerosol that will provide the long laser induced plasma. This number, γ, was determined in a previous section to be 1.6×10^{-4} cm^{-1}. Lastly, for practical reasons, only the shortest possible systems are considered. This means that the laser intensity on the last optical component must be as high as practical, i.e., equal to the damage threshold, $I_{dam} = 0.2 \times 10^9$ watts/cm^2.

Figure (9) is a plot of the intensity of a focussed Gaussian beam as it leaves the lens, converges to a focal region, and then expands. The horizontal axis is distance along the optical axis, normalized to a quantity $P_o/I_{dam}\lambda$, that is the lens' focal length, divided by N. In this analysis, the laser power and wavelength occur only as normalization factors for the axial position, so that all actual lengths are directly proportional to laser power and inversely proportional to laser wavelength. The vertical axis is the Gaussian beam intensity normalized to the optical surface damage threshold intensity, which is also the intensity at the lens. The curves are plots of Equation (4a) in which I_o is set equal to I_{dam}, and πa^2 in Equation (4b) is set equal to P_o/I_{dam}. As N increases, the beam behaves increasingly according to geometrical optics.

The breakdown threshold intensity is also shown in Figure (9). Wherever the intensity curves are above the threshold line, laser induced breakdown occurs. For the present choice of a breakdown threshold to damage threshold intensity ratio of 20, breakdown does not occur for N less than 5, and the maximum breakdown length occurs for N equal to six. The exact positions of the end points of the laser induced plasma, for the case in which laser beam

attenuation is negligible, is obtained by setting $I(z')=I_{bd}$ in Equation (4a) and solving for z'. The result is

$$z'_{2,1} = \frac{1}{N}\left(\beta \pm \sqrt{\alpha\beta-\beta^2/N^2}\right) \tag{6a}$$

$$z'_2 - z'_1 = \frac{2}{N}\sqrt{\alpha\beta-\beta^2/N^2} \tag{6b}$$

$$\alpha = I_{dam}/I_{bd} < 1,\ \beta = N^2(1+N^2)^{-1} \tag{6c}$$

where z_1' is the beginning of the laser induced plasma, z_2' is the end, and $z_2'-z_1'$ is the length of the laser induced plasma. Equation (6b) may be solved computationally for the maximum value of plasma length. For a damage threshold of 0.2 $GWcm^{-2}$ and a breakdown threshold of 4.0 $GWcm^{-2}$, the maximum normalized plasma length is .05 for a value of N equal to six. The corresponding value of the maximum laser induced plasma length, for a 0.5GW, 1.06 micron laser pulse, is .05 $P_0/I_{dam}\ \lambda$ which equals 11.8 meters. The lens focal length for this case is 39.3 meters.

Figure (9) may be used to predict laser induced plasma lengths up to 12 meters since the attenuation length for the laser beam in the aerosol contaminated air is at least 64 meters. No assumed values of any experimental parameters are used in the graph's construction, except that the beam intensity at the lens is kept constant as N varies. This graph is totally inadequate, however, for predicting the 100 times longer maximum breakdown length of the 50GW laser.

Figure (10) is a set of intensity curves that may be used to determine laser produced plasma lengths in cases where laser beam attenuation cannot be neglected. This figure contains an assumed value of α of .05 (Equation (6c)), and it makes use of the experimental procedure of allowing the beam to converge in a zero attenuation atmosphere and entering the attenuating region at a value of intensity equal to I_{bd}. To generate the curves of Figure (10), each curve of Figure (9) is translated to the left by an amount, z_1', (See Equation (6a).) such that $z'=0$ in Figure (10) is the beginning of the laser induced plasma for each value of N. The far end of the plasma is found by

equating the translated intensity function including attenuation to I_{bd} and solving for a value of z' greater than zero. The equation to be solved is

$$I_{bd} = \frac{I_{dam}\,\beta\, e^{-\gamma z'\delta}}{(Nz' - \sqrt{\alpha\beta-\beta^2/N^2})^2 + \beta^2/N^2} \qquad (7a)$$

where γ is the laser beam attenuation constant in cm^{-1} and the axial position normalization factor, δ, is given by

$$\delta = P_o/I_{dam}\lambda \ . \qquad (7b)$$

Figure (10) permits Equation (7a) to be solved graphically. Equation (7a) is rearranged as shown in Equation (7c):

$$\frac{1}{\alpha}\, e^{\gamma z'\delta} = \frac{\beta}{(Nz' - \sqrt{\alpha\beta-\beta^2/N^2}) + \beta^2/N^2} \ . \qquad (7c)$$

The right hand side of this equation produces the intensity curves of Figure (10). The left hand side graphs as straight lines through the point z'=0 and $I(z')/I_{dam}$=20. For a given attenuation constant, γ, the straight line, $(\frac{1}{\alpha}\, e^{\gamma\delta z'})$ is drawn on the graph and the intersections of this line with the intensity curves determine the normalized position of the far end of the laser induced plasma for the various values of N. The actual length of the breakdown plasma is found by multiplying the normalized length by δ.

The exponential function corresponding to γ =(64 meters)$^{-1}$ and P_o=0.5GW is shown in Figure (10). It intersects the N=6 intensity curve at z'=.0445. The attenuation of the laser beam by the aerosol causes a 10% reduction in the length of an approximately 11 meter long laser induced plasma. The exponential function corresponding to the the same attenuation constant and P_o=50GW is also shown. The breakdown length for this laser is maximized by selecting the intensity function that intersects the exponential as far to the right as possible. The intensity function for N=16 meets this requirement and the corresponding values of z' and plasma length are .015 and 354 meters. The lens for this case has a focal length of 1470 meters.

The values for laser induced plasma lengths computed in this section represent the following idealizations: (i) Lens aberrations are neglected. (ii) A perfect Gaussian beam is assumed. (iii) Attenuation by "clean air" is neglected, as well as distortion of the beam by atmospheric fluctuations. Therefore the breakdown plasma lengths computed here are the maximum values possible for the passive, spherical optical systems considered. On the other hand, these computations should serve as starting points for more sophisticated computations and theories.

CONCLUSIONS

There are four contributions reported here. The first is the measurement of the laser breakdown threshold for 1.06 micron radiation in air containing black powder smoke aerosols. The value of the threshold is measured to be 4.0×10^9 watts/cm^2, and within the experimental error of 15% is the same for 60 nanosecond and 4 nanosecond pulses. The second contribution is an estimate of the attenuation constant of the aerosol for the 1.06 micron laser beam in the regime of aerosol densities where the long laser produced plasmas are produced. This attenuation constant is estimated to be $(64 \text{ meters})^{-1}$ at the low end of this density range. The third contribution is a method based on light scattering for determining the attenuation constant of an aerosol whose density is decreasing exponentially with time. This method has the advantage of not requiring transmitted light measurements or absolute intensity measurements. The attenuation constant is determined from the time of occurrence of the maximum of the scattered intensity.

The fourth contribution is a prescription for maximizing laser induced plasma lengths under idealized conditions and a graphical system for determining such plasma lengths. A graphical solution finds the Fresnel number, for a given laser breakdown threshold and laser damage threshold on the focussing optics, that maximizes a normalized plasma length. The actual laser induced plasma length is the product of this normalized length, the laser power divided by the laser wavelength, and the damage threshold. The maximum lengths of laser induced breakdown plasmas calculated in this way are of the order of hundreds of meters for lasers existing now at NRL. These lengths are extremely encouraging, even with the realization that the

calculation assumes ideal conditions. One area of doubt remains: It is not known for sure if a high voltage electric discharge will follow the path of an optimized laser induced plasma. All laser guided electric discharge experiments have been conducted with laser pulses that deposit an energy density much higher than would be deposited with a maximally long discharge.

ACKNOWLEDGMENTS

Ensign Kevin Reilly assisted with data collection on each of these experiments. The idea of using concrete casting tubing for the experiment chamber and the design of the chamber were contributed by Stewart Hauver. The construction and design details of the chamber were shared by Edward Laikin, William Dolinger, and Wayne Somerville. The original idea of using black powder to generate the aerosol for enhancing the laser/atmosphere interaction was contributed by Edward Laikin. The authors are also grateful to Lt. Cmdr. Jeff Perin for his interest, his indefatigable enthusiasm, and his encouragement, all directed to toward making long laser guided electric discharges and eventually shipboard antennas.

The very high intensity laser experiment was performed using the PHAROS II laser at NRL, and with the assistance of Nicolas Nocerino, Dr. Stephen Obenschain and Dr. Barrett Ripin.

The handling of ragweed pollen was undertaken after receiving advice and instruction from Dr. Paul C. Turkeltaub of the National Institutes of Health.

This work was supported by the Office of Naval Research and by the Naval Sea Systems Command.

TABLE I

This table is a condensed version of some of the data presented in Appendix I: The average values of laser induced plasma length per unit of laser pulse energy are indexed with respect to time interval and f-number to show the spread in the data the maximum and minimum values are also shown.

f-number	T=10 sec	10<T<100 sec	100<T<1400 sec	1400<T<10^4 cm
138	No Data	2.45 Avg. cm/J 1.67-3.02	3.4 Avg. cm/J 2.62-4.08	1.46 Avg. cm/J .83-2.2
235	5.04 Avg. 1.88-8.7	3.96 Avg. 3.27-4.88	7.8 Avg. 6.45-9.45	6.06 Avg. 4.51-8.98
361	3.6 Avg. 2.85-4.32	2.87 Avg. 2.2-3.54	11.1 Avg. 9.9-13.5	5.24 Avg. 3.5-6.7

TABLE II

Parameters of the three optical systems used.

f-Number	Lens Focal Length, L_f	Beam Phase Surface Curvature, R_o	Beam Radius at lens, a	Fresnel Number, N
138	5m	5.9m	2.1cm	233
235	7.5m	9.4m	2.0cm	127
361	10m	13.7m	1.9cm	78

APPENDIX I

This appendix contains the data from the Nd/glass laser induced plasma experiment that is shown in Figures (1) and (2). The column titles represent the shot number, the focal length of the laser focussing lens, the f-number for that lens, the time interval after the ignition of the black powder that the laser was fired, the energy of the laser pulse, the length of the laser induced plasma, and the length of the plasma per unit energy of the laser pulse.

Shot No.	F.L.	f-num	Time	Energy	Length	L'
142	10 m	361	30 sec	29.7 J	105 cm	3.54 cm/J
143	"	"	300	30.7	305	9.93
144	"	"	1145	31.5	306	9.71
4	"	"	300	19.5	264	13.54
5	"	"	10^3	15	170	11.33
6	"	"	30	15.8	35	2.22
8	"	"	100	24	130	5.42
145	"	"	3000	30.7	135	4.40
147	"	"	3564	15	100	6.7
148	"	"	3847	25.5	110	4.31
150	"	"	10^4	17.9	65	3.63
151	"	"	10^4	21.8	80	3.67
152	"	"	10^4	27	95	3.52
3	"	"	10	15.8	45	2.85
7	"	"	10	17.6	76	4.32
16	"	"	∞	25.5	156	6.12
23	"	138	300	21	55	2.62
24	"	"	1000	21	62	2.95
25	"	"	1200	18	60	3.33
26	"	"	1360	9.8	40	4.08
32	"	"	300	16.5	54	3.37
34	"	"	300	9.75	37	3.97
27	"	"	2760	9.0	<20	<2.27
28	"	"	2965	15	<20	<1.33

Shot No.	F.L.	f-num	Time	Energy	Length	L/E
29	5.0 m	138	3150 sec	24 J	<20 cm	<.83 cm/J
35	"	"	100	9.5	35	3.68
36	"	"	100	20	57	2.83
22	"	"	30	21	35	1.67
30	"	"	75	14.25	43	3.02
31	"	"	30	13.5	36	2.67
44	7.5	235	320	24	165	6.88
45	"	"	1030	24.5	158	6.45
46	"	"	1200	15	111	7.40
55	"	"	300	18	149	8.28
61	"	"	320	10.5	88	8.38
47	"	"	1380	9.8	93	9.49
52	"	"	100	22.5	154	6.84
60	"	"	120	10.5	90	8.6
51	"	"	30	24	117	4.88
62	"	"	30	8.3	33	3.98
48	"	"	2835	9.8	88	8.98
49	"	"	3040	15.8	74	4.68
50	"	"	3240	19.5	8.8	4.51
57	"	"	30	16.5	54	3.27
50	"	"	30	18.	67	3.72
43	"	"	10	24	45	1.88
53	"	"	10	15	68	4.54
59	"	"	10	9.8	85	8.7

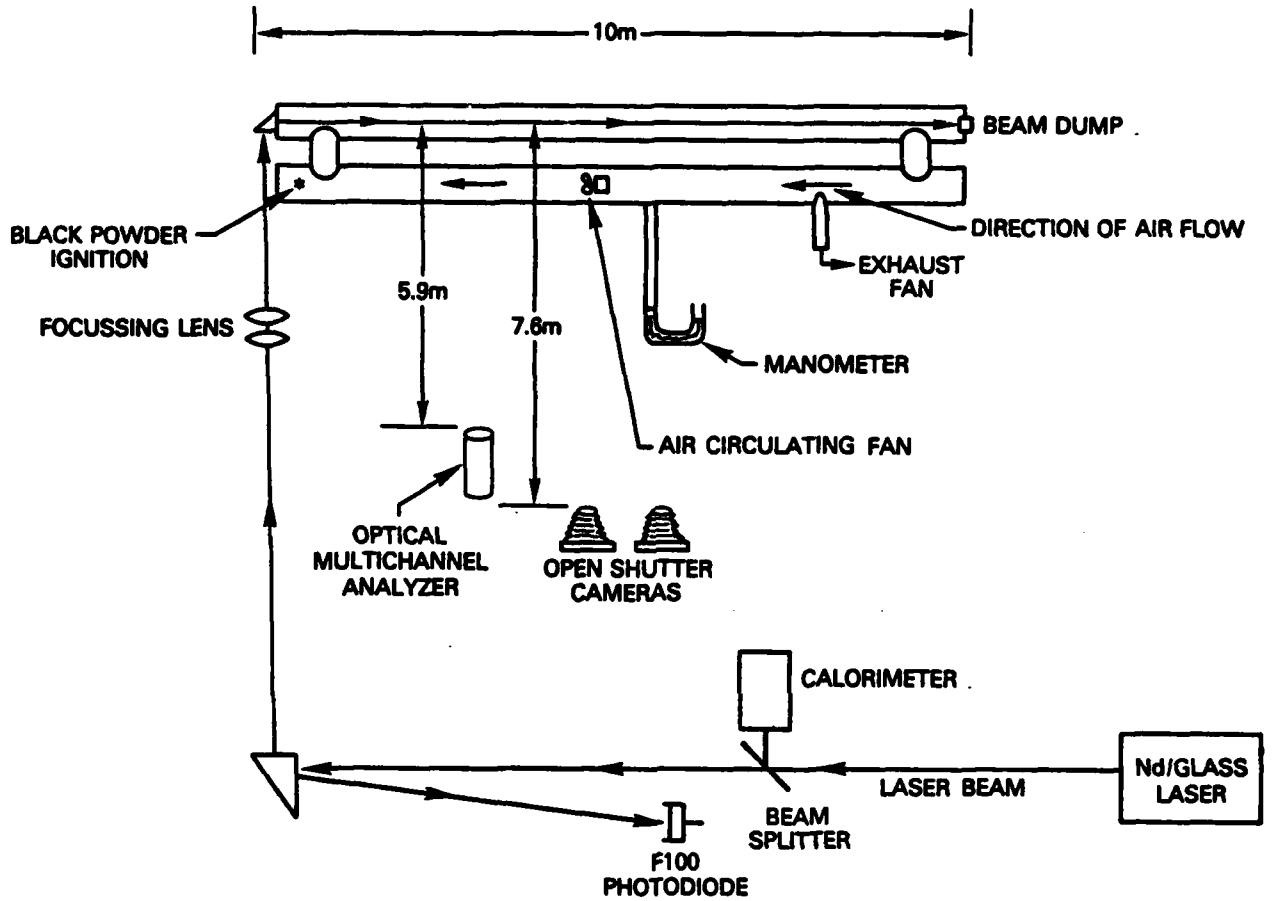

Figure 1. Schematic diagram of the laser induced plasma experiment. The Nd/glass laser is monitored and focussed into a 50 cm diameter, 10 meter long, controlled atmosphere tube. The length of the resulting laser induced plasma is determined from open shutter camera photographs. The black powder aerosol density is inferred from scattered light measured by an optical multichannel analyzer.

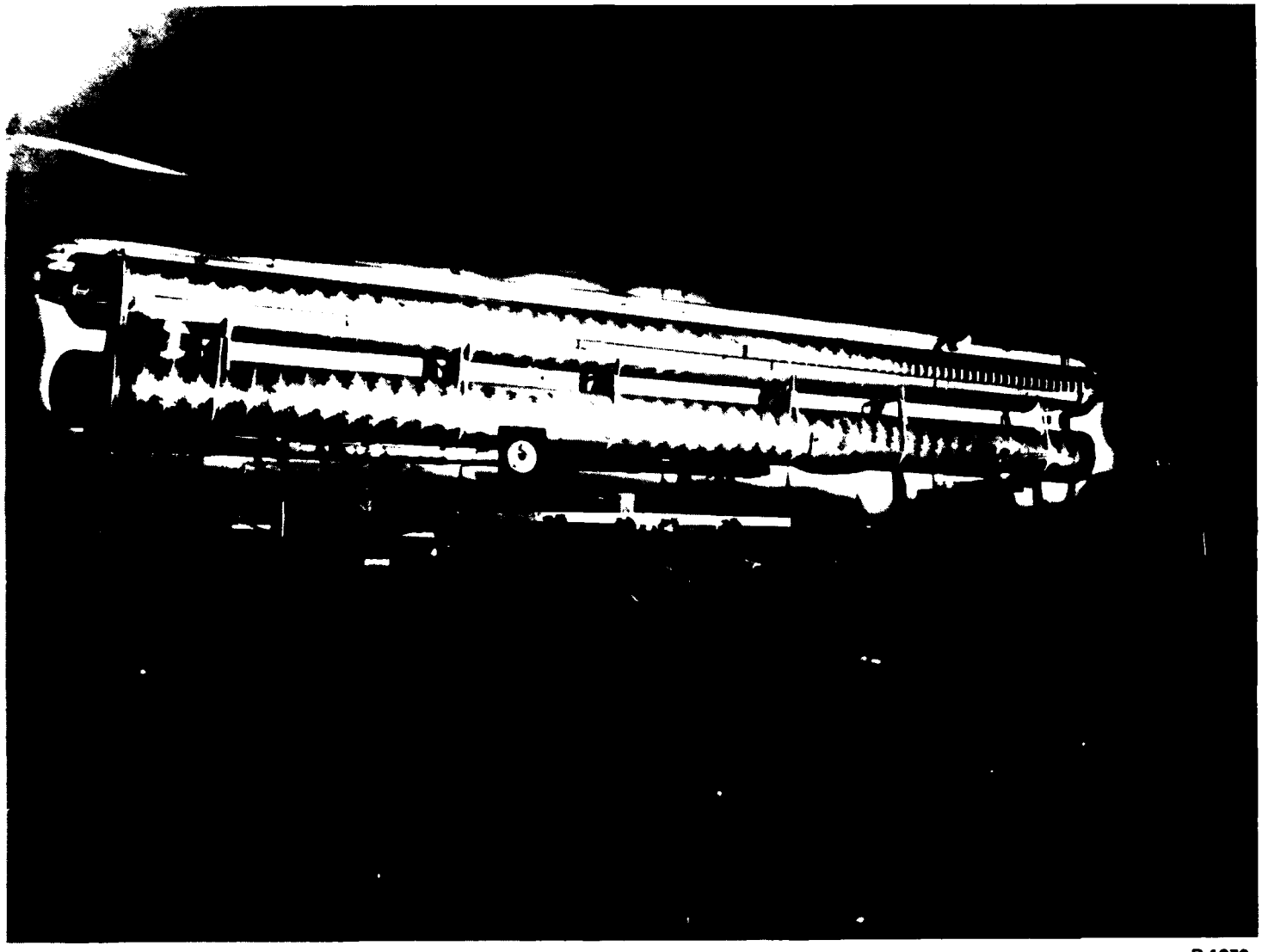

R-1070

Figure 2. Photograph of the experiment chamber in which the Nd/glass laser induced plasmas are created. The scale marks above the window in the upper tube are 10 cm apart.

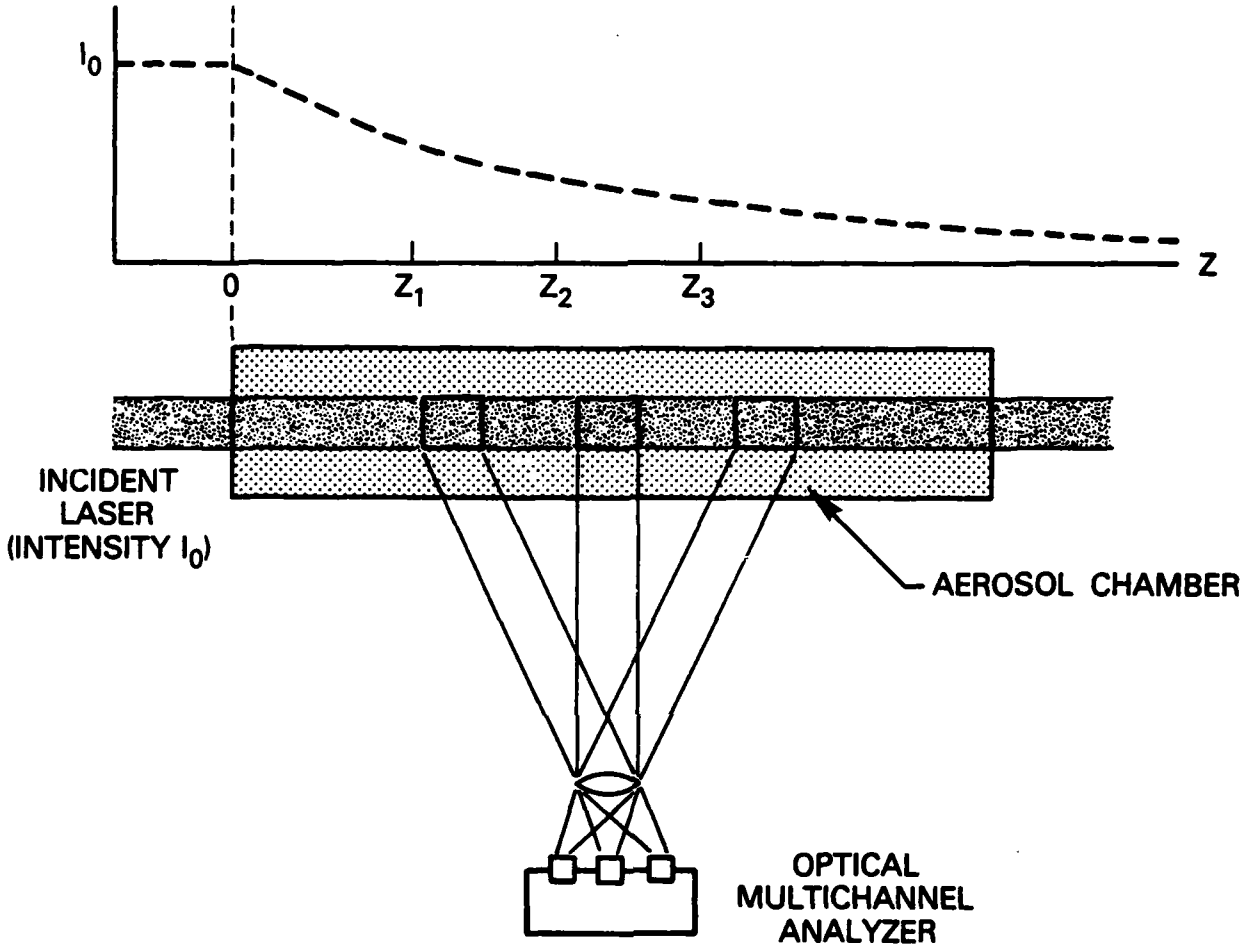

Figure 3. Schematic diagram of the argon ion laser/aerosol scattering system for measuring the product of aerosol density and total scattering cross section. The laser is incident from the left and is attenuated by the presence of the aerosols, as shown in the upper part of the diagram. Light scattered by aerosols in small volumes around z_1, z_2, and z_3 are scattered into the OMA. The scattered light is recorded for several density decay times.

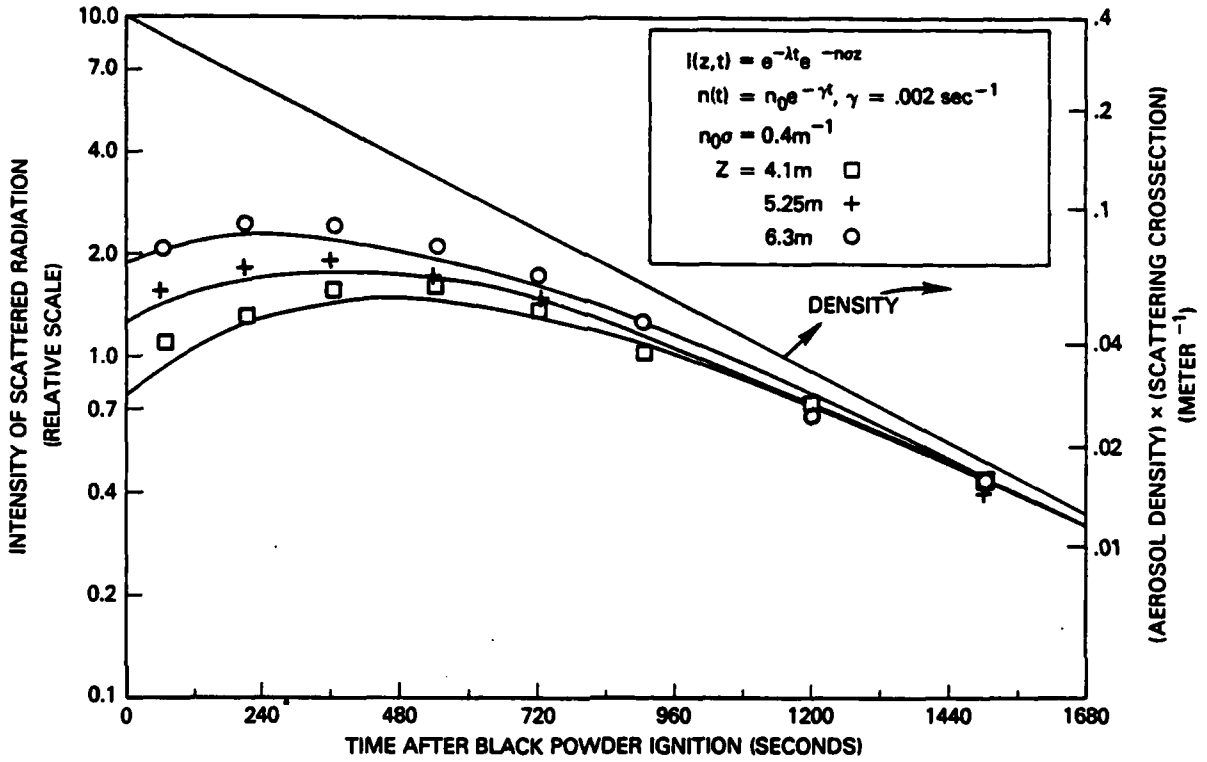

Figure 4. Comparison of the theoretical and the measured values of light scattered by the aerosol from the argon ion laser beam at three positions along the optical axis.

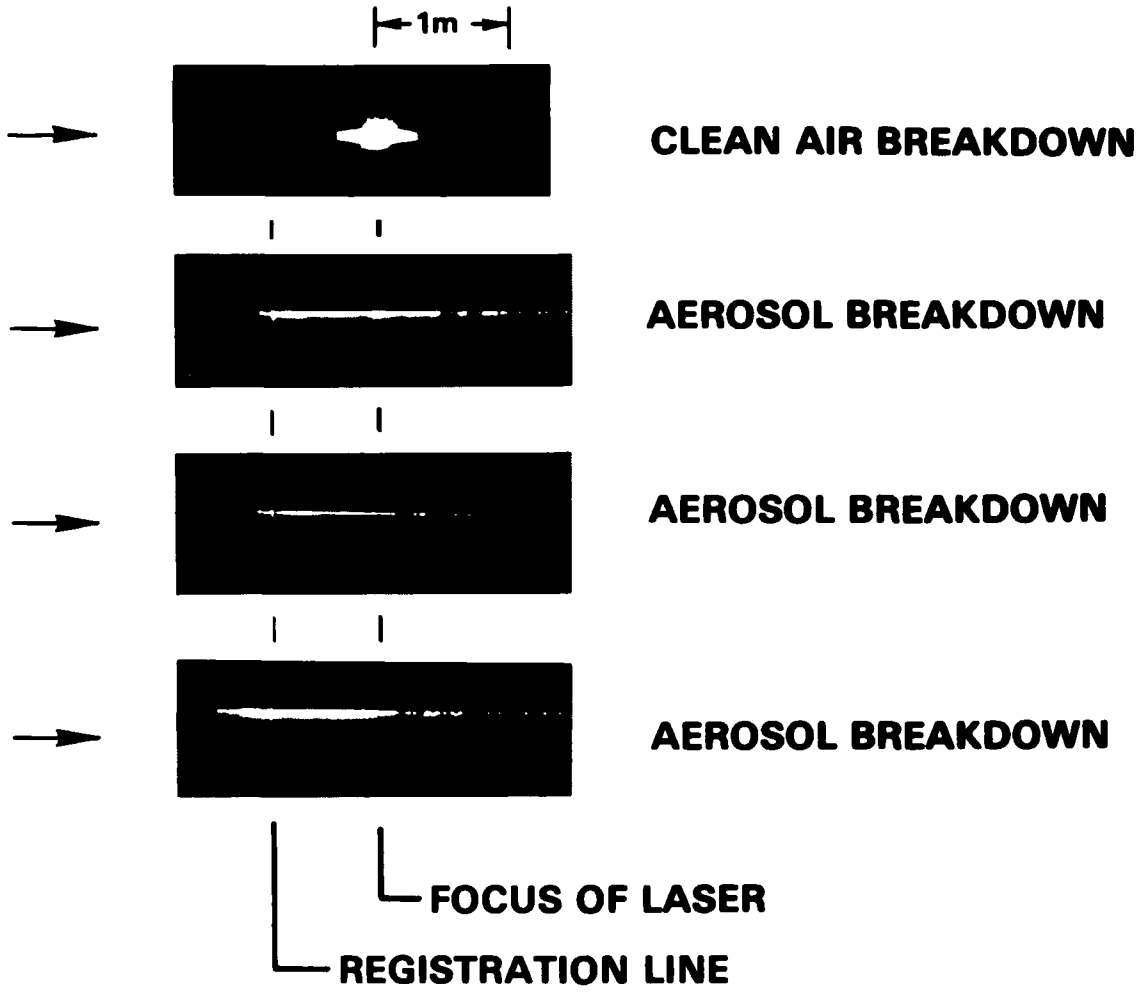

Figure 5. Photographs of laser induced plasmas in the experiment chamber. The top plasma is in clean air and is used to locate the laser focal point. The three other plasmas are initiated on aerosol particles. The figure shows that the laser induced plasmas, at least on the average, extend as far beyond focus as they do in front of focus.

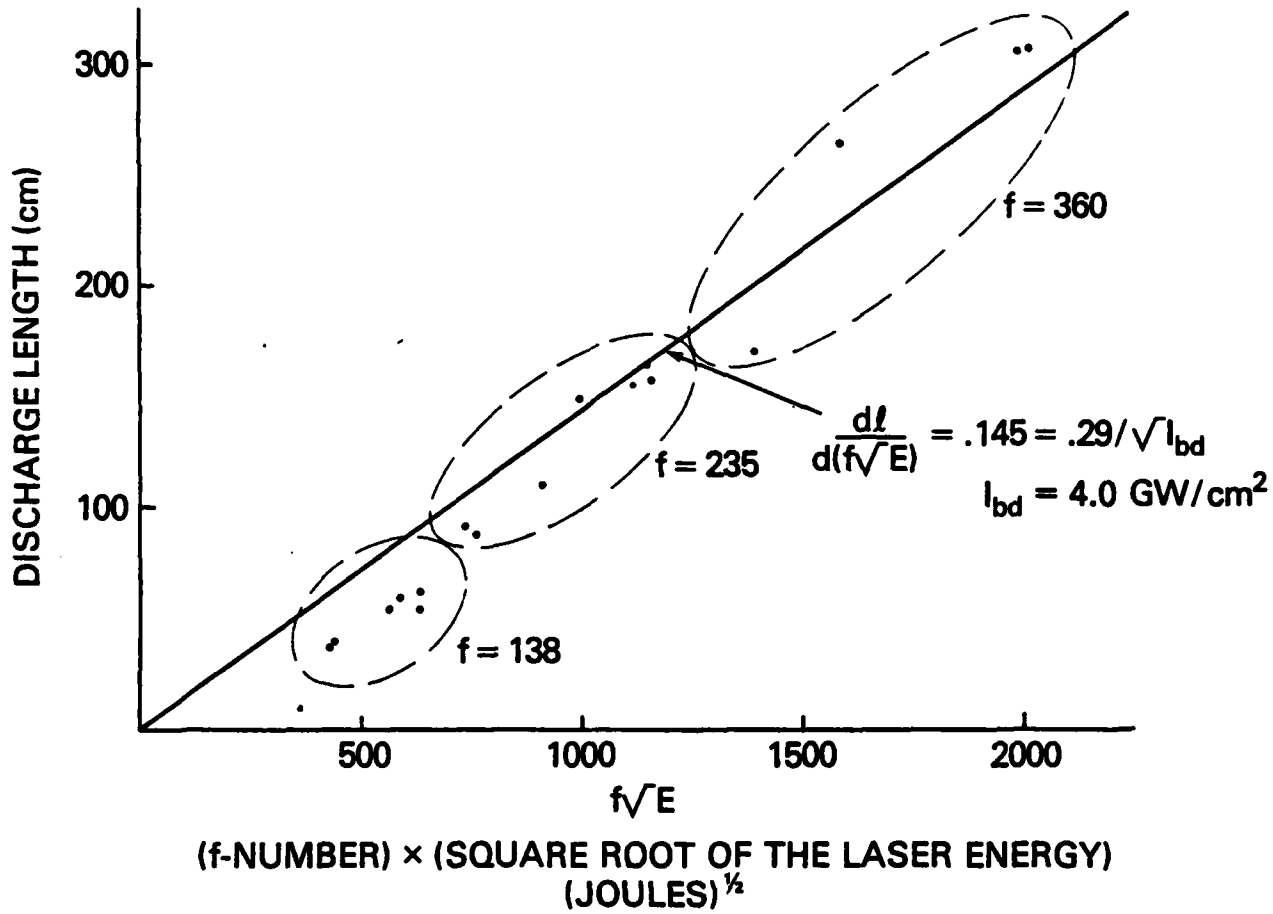

Figure 6. Plot of the lengths of the laser induced plasmas versus the product of their f-number and the square root of the energy of their laser pulses. The dashed line is the best straight line fit to the data points. The slope of this line is used to determine the intensity threshold for laser induced plasmas.

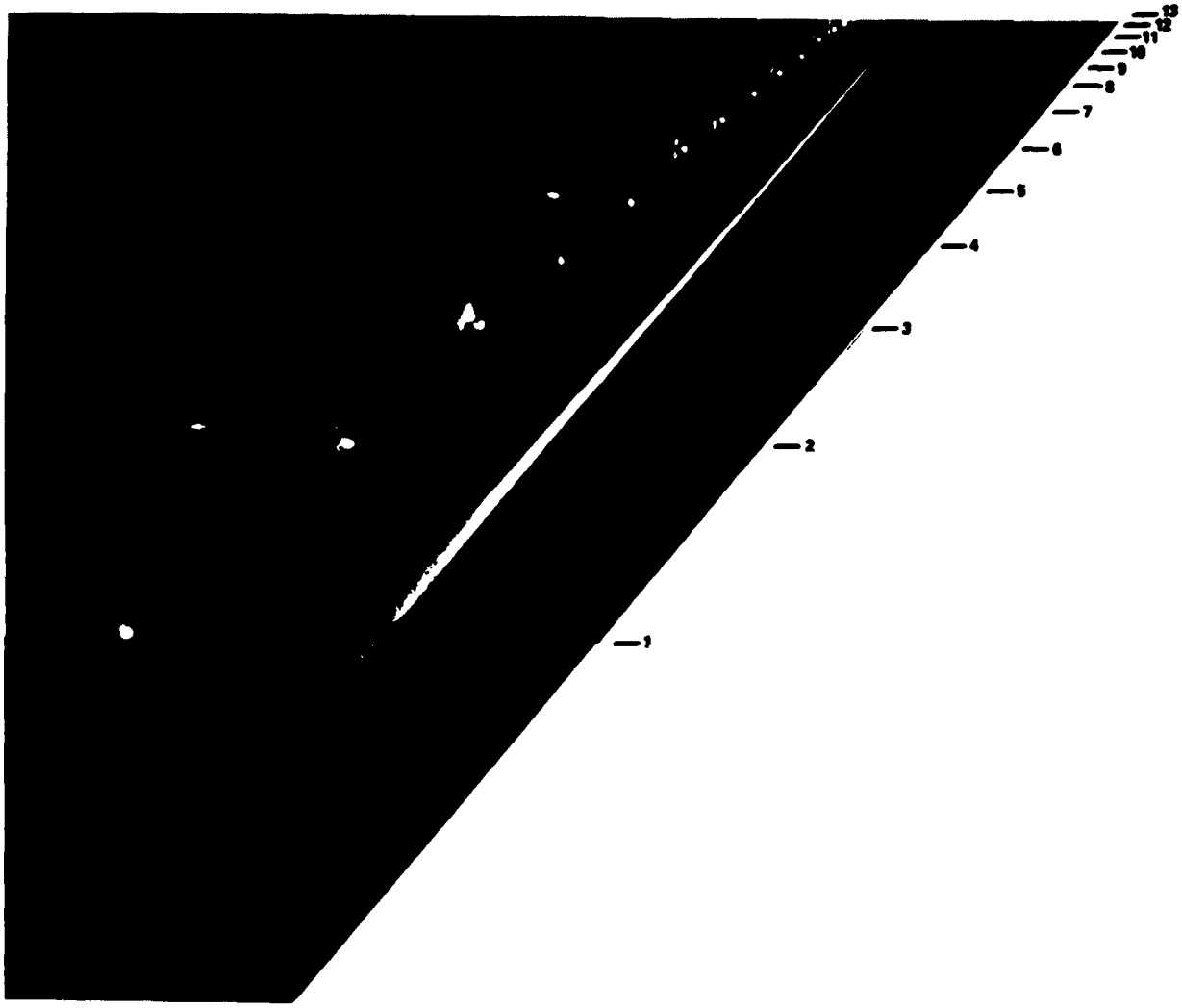

Figure 7. Photograph of a 10 meter long laser induced plasma created by a 200 Joule, 4 nanosecond, laser pulse. Lights, one meter apart, are located parallel to the plasma for scaling purposes.

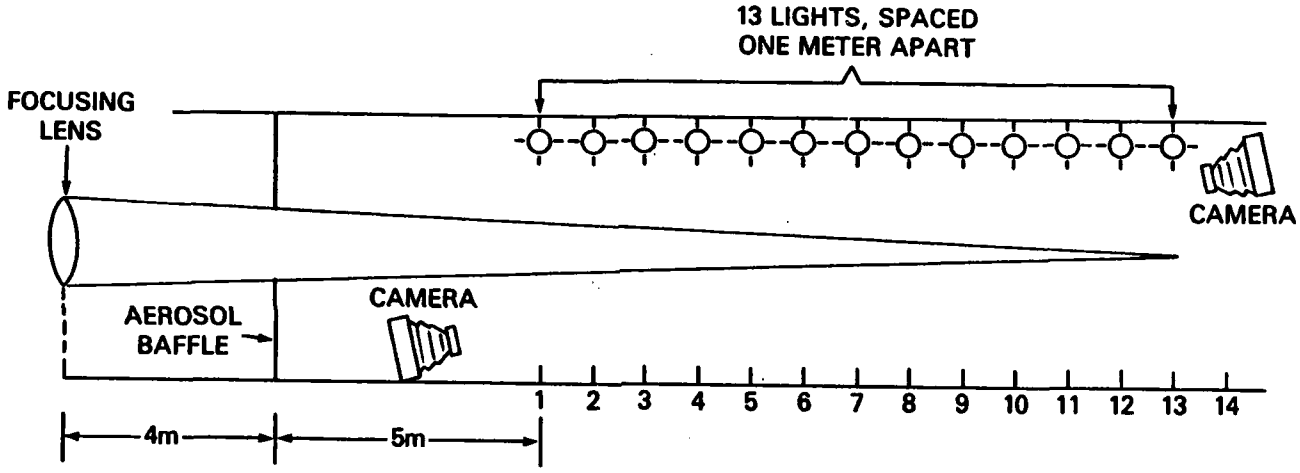

Figure 8. Schematic diagram of the 10 meter laser induced plasma experiment.

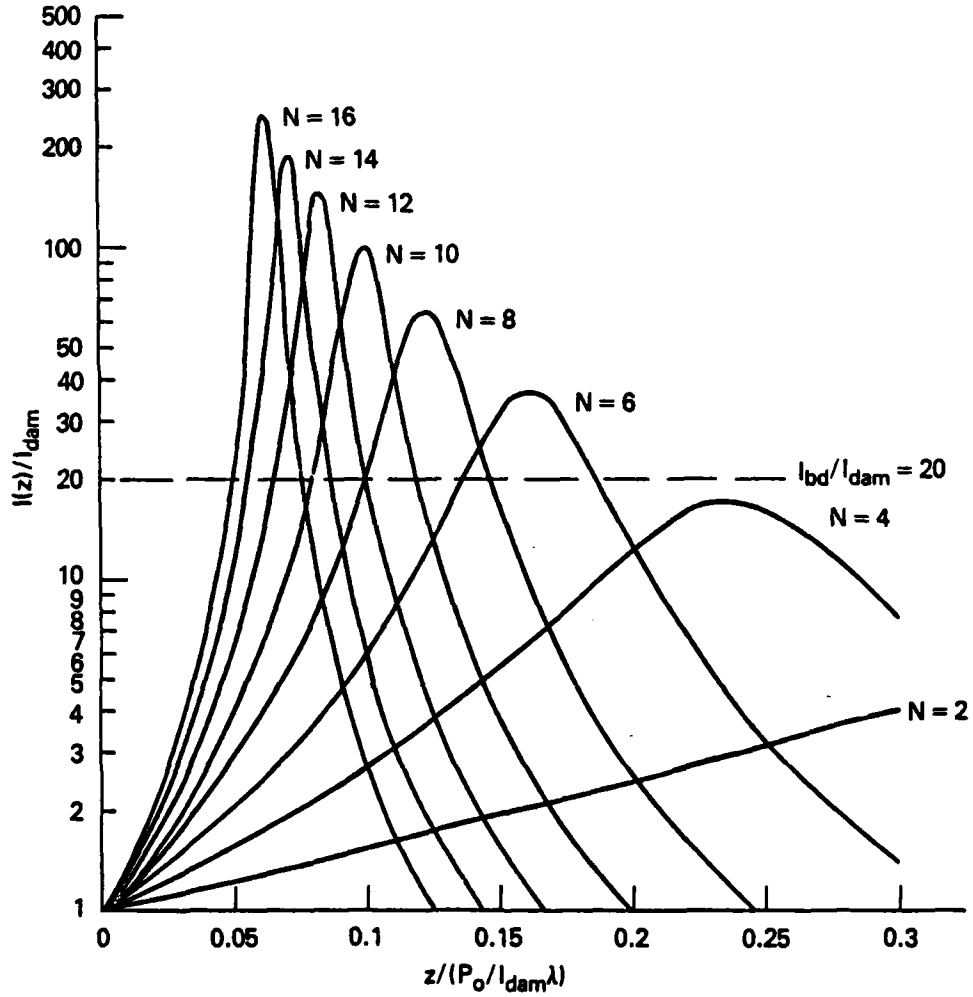

Figure 9. Plot of the intensity along the optical axis of a focussed Gaussian beam for various values of Fresnel number. The intensity is normalized to the intensity at the lens, and the axial position is normalized to a number that is related to focal length. The breakdown threshold is also shown.

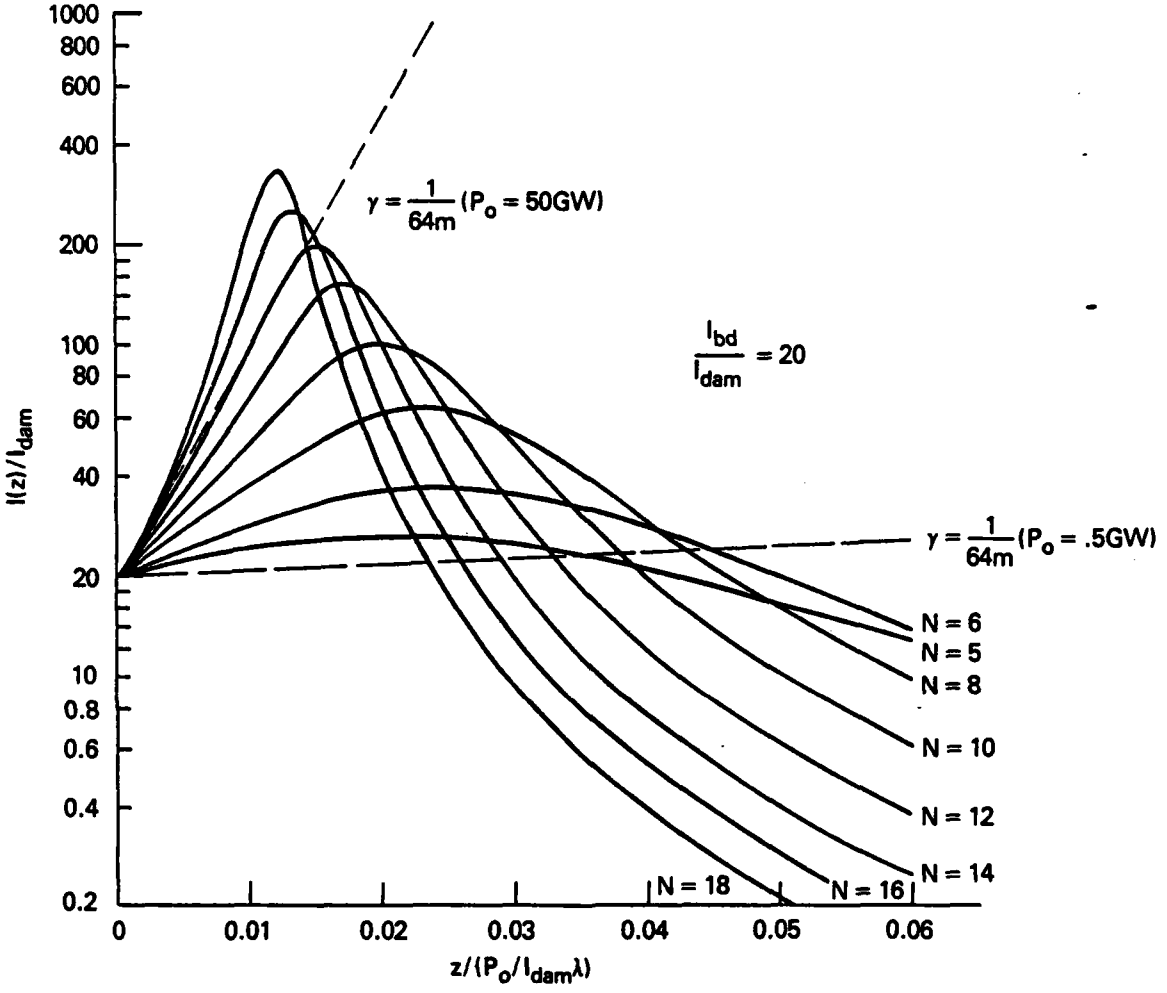

Figure 10. Plots of the intensity along the optical axis of a focussed Gaussian beam for various values of Fresnel numbers and with the position coordinate of each curve translated such that $I(z'=0)=I_{bd}$. The laser produced plasma channel for all curves begins at $z'=0$. The straight lines represent laser beam attenuation, and the intersections of the attenuation lines and the intensity curves define the far ends of the plasma channels.

REFERENCES

1. T.J. Dwyer, J.R. Greig, D.P. Murphy, J.M. Perin, R.E. Pechacek, and M. Raleigh "On the feasibility of using an atmospheric discharge plasma as an RF antenna." IEEE Transactions on AP-S, to be published February (1984). [See also NRL Memorandum Report 4815 (1982)] AD-A115362

2. Tadeusz Urbanski, Chemistry and Technology of Explosives, Vol. III, Pergamon Press, New York (1967), Page 335.

3. Max Born and Emil Wolfe, Principles of Optics, Second Rev. Edition, The Macmillan Company, New York (1964), p. 662.

4. H. Kogelnik and T. Li, "Beams, Modes, and Resonators," in CRC Handbook of Lasers, R.J. Pressley, Editor, The Chemical Rubber Company, Cleveland, OH, (1971).

5. R.F. Fernsler, private communication.

DISTRIBUTION LIST

1. Dept. of the Navy
   Chief of Naval Operations
   Washington, D.C. 20350
   ATTN: Dr. C. F. Sharn (op 987)

2. Commander
   Naval Sea Systems Command
   Department of the Navy
   Washington, DC 20363
   ATTN: NAVSEA/PMS 405 (Capt R.L. Topping)
   P.E. Law, SEA 61X32
   H.J. De Mattia, SEA 61R4
   A.F. Johnson, SEA 05R22
   Dr. D.J. Pastine, SEA 06R

3. Air Force Weapons Laboratory (NTYP)
   Kirtland Air Force Base
   Albuquerque, New Mexico 87117
   ATTN: Maj. James Head
   Dr. David Straw

4. U.S. Army Ballistics Research Laboratory
   Aberdeen Proving Ground, Maryland 21005
   ATTN: Dr. D. Eccleshall (DRDAR-BLB)

5. Ballistic Missile Defense Advanced Technology Center
   P. O. Box 1500
   Huntsville, Alabama 35807
   ATTN: Dr. L. Harvard (BMDSATC-1)

6. B-K Dynamics Inc.
   15825 Shady Grove Road
   Rockville, Maryland 20850
   ATTN: Dr. R. Linz

7. Lawrence Livermore Laboratory
   University of California
   Livermore, California 94550
   ATTN: Dr. R. J. Briggs
   Dr. T. Fessenden
   Dr. W. Barletta
   Dr. D. Prono

8. Pulse Sciences Inc.
   14796 Wicks Blvd.
   San Leandro, CA 94577
   ATTN: Dr. S. Putnam

9. Naval Surface Weapons Center
White Oak Laboratory
Silver Spring, Maryland 20910
ATTN: Dr. C. M. Huddleston
Dr. R. B. Fiorito

10. Office of Naval Research
Department of the Navy
Arlington, Virginia 22217
ATTN: Dr. W. J. Condell (Code 421)

11. Avco Everett Research Laboratory
2385 Revere Beach Pkwy.
Everett, Massachusetts 02149
ATTN: Dr. R. Patrick
Dr. Dennis Reilly

12. Defense Technical Information Center
Cameron Station
5010 Duke Street
Alexandria, Virginia 22314 (2 copies)

13. Naval Research Laboratory
Washington, D. C. 20375
ATTN: T. Coffey - Code 1001
M. Lampe - Code 4792
M. Friedman - Code 4700.1
J. R. Greig - Code 4763 (50 copies)
I. M. Vitkovitsky - Code 4701
W. R. Ellis - Code 4000
S. Ossakow, Supt. - 4700 (26 copies)
Library - Code 2628 (20 copies)
A. Ali - Code 4700.1T
D. Book - Code 4040
J. Boris - Code 4040
S. Kainer - Code 4790
A. Robson - Code 4760
M. Picone - Code 4040
M. Raleigh - Code 4763
R. Pechacek - Code 4763
D.P. Murphy - Code 4763
R.F. Fernsler - Code 4790
J. D. Sethian - Code 4762
K. A. Gerber - Code 4762
G. Joyce - Code 4790
D. Colombant - Code 4790
B. Hui - Code 4790

14. Defense Advanced Research Projects Agency
1400 Wilson Blvd.
Arlington, Virginia 22209
ATTN: Dr. J. Mangano
Lt. Col. R.L. Gullickson

15. Sandia National Laboratories
Albuquerque, New Mexico 87185
ATTN: Dr. Bruce Miller, 4255
Dr. Carl Ekdahl
Dr. M. Mazarakis

16. Naval Air Systems Command
Washington, D. C. 20361
ATTN: Dr. J. Reif, Code AIR-350F

17. U. S. Department of Energy
Washington, D. C. 20545
Office of Fusion Energy, ATTN: Dr. W. F. Dove
Office of Inertial Fusion, ATTN: Dr. Richard L. Schriever
Office of High Energy and Nuclear Physics-ER20:GTN,
ATTN: Dr. T. Godlove

18. AFOSR/NP
Bolling Air Force Base, Bldg. 410
Washington, D. C. 20331
ATTN: Capt. H. Pugh

19. Foreign Technology Division
Wright Patterson AFB, OH 45433
ATTN: Mr. C. J. Butler/TQTD

20. SRI International
333 Ravenswood Avenue
Menlo Park, CA 94025
ATTN: Dr. D. Eckstrom

21. Los Alamos National Laboratory
Los Alamos, NM. 87545
ATTN: Dr. T. P. Starke, M-2

22. G T Devices
5705 General Washington Drive
Alexandria, VA 22312
ATTN: Dr. D. A. Tidman
Dr. S. A. Goldstein
Dr. R. Hubbard

23. Directed Technologies Inc.
1226 Potomac School Road
McLean, Va 22101
ATTN: Dr. Ira F. Kuhn, Jr.


FILMED